Journal of Physics: Conference Series **220** (2010) 012008 doi:10.1088/1742-6596/220/1/012008

Modeling transient aspects of coherence-driven electron transport

A Prociuk, H Phillips, and B D Dunietz*

The University of Michigan, Ann Arbor, Michigan 48109

E-mail: bdunietz@umich.edu

Abstract. Non-equilibrium Green's function formalism (NEGF) by employing time-dependent (TD) perturbation theory is used to solve the electronic equations of motion of model systems under potential biasing conditions. The time propagation is performed in the full frequency domain of the two time variables representation. We analyze transient aspects of the resulting conductance under effects of applied direct-current and alternating current potentials. The coherence induced response dependence on different aspects of the applied perturbation is resolved in time and analyzed using calculated TD distributions of the current operator.

1. Introduction

The study of electron and energy transport through molecular and nanoscale systems is drawing a large volume of research attention.[1, 2, 3, 4, 5, 6, 7, 8, 9, 10, 11, 12, 13, 14, 15, 16, 17, 18, 19, 20, 21, 22, 23, 24, 25, 26, 27, 28, 29, 30, 31, 32, 33, 34, 35, 36, 37, 38, 39, 40, 41, 42, 43, 44, 45] The appeal stems mainly from prospects with which nanotechnology is associated and requires understanding of the complex physics of electron transport (ET) processes at the atomic and electronic structure levels.[46, 47, 48, 49, 50, 51, 52, 53, 54, 55, 19, 20, 56] Computational modeling of the transport plays a crucial role in this research, where *insight at the most fundamental level is achieved.* While the main focus of ET studies has been the steady state, recent technological advances are promising to shift this.[57, 58] Due to these advances, the modeling of the temporal resolution of electron transport becomes essential.[59, 60, 61, 62, 63, 64, 65, 66]

In general, the study of systems, where quantum interferences affect the ET, requires resolving the time-dependent (TD) conductance. This includes the study of transient conductance, where the system still evolves to a steady state. TD studies revealed interesting quantum effects associated with photo-assisted conductances in mesoscopic systems, such as absolute negative conductance, Coulomb blockade, and Kondo effects driven by alternating-current (AC) fields.[67, 48, 49, 50, 55, 56] Other studies highlight the importance of transient effects, where the non-equilibrium nature of ET determines the switching rate and efficiency of the transport. Time-resolved THz spectroscopy was used to study carrier dynamics within nano-crystal arrays, where the inter-dots coupling has been varied by modifying the length of the surface bound ligand.[57] The importance of considering the dynamics of ET for analysis of experimental data is also demonstrated by Raman spectra of molecular-scale junctions that relate the conductance to spectroscopic changes. [68, 69, 70, 71, 72]

The dynamics of electron transport is greatly complicated by inherent dissipative aspects. The complexity of the ET due to quantum dephasing is reflected even for model systems of non-interacting electrons in bulk-coupled systems driven by TD potentials.[73, 74, 75, 76, 77, 78, 79, 80, 81, 82, 66] Recent computational studies that analyze currents under TD applied potentials include approaches based on TD-DFT,[83, 84, 85, 59, 61, 86, 60, 87, 88, 89] density matrix equations with Floquet representation or quantum master equations,[90, 91, 92, 93, 94, 66] Floquet scattering matrix approach,[95, 96] and Keldysh non-equilibrium formalism.[97, 98, 99, 62, 100, 101, 66] Keldysh Green's function (GF)-based expansions[102, 103, 104, 105, 106] provide for a rigorous route to treat electron dynamics in biased systems[97] and are used below to analyze quantum interferences affecting the transient transport.

We are implementing a dynamical approach based on Keldysh formalism to study ET. The effect of the bulk is to broaden and shift the electronic DOS resulting with an energy distribution of the electronic density matrix ($\rho(E)$). This may involve broadened states that couple the two leads providing an efficient transport channel. The Keldysh NEGF formalism relates a coupled electronic system experiencing a TD perturbation to its thermally equilibrated initial state. In this approach, thermal coupling to the bulk is represented by the imaginary part of the time ordered contour that is used to define the electronic equations of motion (e.o.m.). Broadening effects due to the electrodes' coupling are treated consistently, where the bulk-induced manifolds of junction's states are directly propagated. The electronic density of the coupled system can be extracted from these equations.

Most descriptions of dynamic transport that are GFs-based formalisms follow the seminal work of Jauho et al.,[97] where system partitioning for the unperturbed state is employed. In this picture the system's components are each kept in thermal isolation up to switching on the perturbation. Initial state designation, as reflected from model-partitioning, however, may affect the evolution of the system to steady state. Transient effects, therefore, can reliably be treated only by a non-partitioning scheme, which is fully and consistently equilibrated. Below we employ the more consistent approach within the Keldysh formalism, where the full equilibration of the unperturbed device with the electron baths is included.[107] The importance of the partition-free approach was highlighted in several recent real time-based propagations.[59, 60, 66]

2. Approach

2.1. The Kadanoff-Baym electronic equations of motion

The central quantities of Keldysh and NEGF formalisms are the one-body Green Functions (GF)[104, 106, 108], which are functions of two space-spin and time coordinates ($x = \vec{x}, t$), with time variables expressed on the Keldysh contour (KC). The GFs are defined by pair of field operators ($\hat{\Psi}(\vec{x})$ and $\hat{\Psi}^{\dagger}(\vec{x'})$) at times t and t' respectively:

$$G(x,x') \equiv -i\frac{Tr[\hat{U}(t_0 - i\beta, t_0)\hat{\mathcal{T}}_C[\hat{\Psi}_H(x)\hat{\Psi}^{\dagger}_H(x')]]}{Tr[\hat{U}(t_0 - i\beta, t_0)]}. \tag{1}$$

In the Heisenberg picture, these operators take the form:

$$\hat{\Psi}_H(x) = \hat{U}(t_\circ, t)\hat{\Psi}(\vec{x})\hat{U}(t, t_\circ) \tag{2}$$

where $U(t,t')$ propagates the fully time dependent hamiltonian from t' to t on the KC. For the special case of a time independent Hamiltonian, $U(t,t') = e^{-i\hat{H}(t-t')}$ and $G(x,x')$ reduces to a GF of the time difference $G^0(\vec{x},\vec{x'};t-t')$. The superscript, zero, is used to denote a GF corresponding to the Hamiltonian without a time dependent contribution. The contour ordering operator, $\hat{\mathcal{T}}_C$, can be expanded, allowing the GF to be expressed as a sum over two types of GFs related to the relative positions of the two time variables on the contour:

$$G(x,x') = \theta(t,t')G^{>}(x,x') + \theta(t',t)G^{<}(x,x'), \tag{3}$$

where the step function, $\theta(t,t')$, is as usual zero for t appearing before t' on the Keldysh contour and one otherwise. The contour, therefore, defines 7 types of GFs that each solve a different electronic equation of motion (e.o.m.) (Kadanoff-Baym (K-B) equations). The K-B equations are related to each other through analytic continuation as set forth by the KC.[105]

We start with the K-B equation for the case of non-interacting electrons expressed by the lesser GF ($G^<$):

$$\left[i\mathbf{S}\frac{\partial}{\partial t} - \mathbf{h}(t)\right]\mathbf{G}^<(t,t') = 0 \tag{4}$$

$$-i\frac{\partial}{\partial t'}\mathbf{G}^<(t,t')\mathbf{S} - \mathbf{G}^<(t,t')\mathbf{h}(t') = 0, \tag{5}$$

where $h(t)$ is the TD electronic Hamiltonian and S is the overlap of the orbitals used in the expansion. Note that for this equation, we assume that t and t' are both on the real branch of the KC. We are neglecting electron-electron SE interaction terms. The complete one-body Hamiltonian takes the following form:

$$h(x) = h_0(\vec{x}) + v(x), \tag{6}$$

where $v(x)$ is a time dependent external potential acting on the electrons and $h_0(\vec{x})$ represents the electron kinetic energy and electron nuclear attractions. We combine equations 4-5 by rewriting in terms of the time average and correlation variables: $\bar{t} \equiv \frac{t_1+t_2}{2}$ and the $\Delta t \equiv t_1 - t_2$:

$$\frac{\partial}{\partial \bar{t}}\mathbf{G}^<(\bar{t},\Delta t) = i\left[\mathbf{G}^<(\bar{t},\Delta t)\mathbf{h}(\bar{t}-\frac{\Delta t}{2}) - \mathbf{h}(\bar{t}+\frac{\Delta t}{2})\mathbf{G}^<(\bar{t},\Delta t)\right]. \tag{7}$$

2.2. Mixed time-frequency space representation

Pure time-domain representations require using sufficiently large clusters to reliably treat conductance through a device region. In the frequency domain on the other hand, self-energy expressions can use a cluster model to effectively represent an open system. Frequency domain bulk-self energy (SE) models are used below to represent the dissipative effect of coupling to the electrodes. Earlier, we analyzed the convergence of transport calculations using bulk-coupling DFT-based SEs with their model size.[109] We introduce the frequency variable by Fourier transforming over Δt using a generalized transform operator ($\mathcal{F}$):

$$\begin{aligned}\mathcal{F}[f(\Delta t)] \equiv \int_{-\infty}^{\infty} d(\Delta t)\left[e^{i(\bar{\omega}+i\eta)\Delta t}\Theta(\Delta t) + e^{i(\bar{\omega}-i\eta)\Delta t}\Theta(-\Delta t)\right]f(\Delta t)\\ \equiv f_1(\bar{\omega}) + f_2(\bar{\omega}) \equiv f(\bar{\omega})\end{aligned} \tag{8}$$

where $\eta \to 0^+$, leads, when applied on $G^<(\bar{t},\Delta t)$, to

$$\mathbf{G}^<(\bar{t},\bar{\omega}) = \mathbf{G}_1^<(\bar{t},\bar{\omega}) + \mathbf{G}_2^<(\bar{t},\bar{\omega}), \tag{9}$$

with

$$\begin{aligned}\mathbf{G}_1^<(\bar{t},\bar{\omega}) &= \int_{-\infty}^{\infty} d(\Delta t) e^{i(\bar{\omega}+i\eta)\Delta t}\Theta(\Delta t)\mathbf{G}^<(\bar{t},\Delta t) \qquad \text{and}\\ \mathbf{G}_2^<(\bar{t},\bar{\omega}) &= -\mathbf{G}_1^{\dagger<}(\bar{t},\bar{\omega}).\end{aligned} \tag{10}$$

The use of the two branches, where Θ is the step function, ensures that the transformed function approaches zero as Δt approaches $\pm\infty$. The resulting transformed e.o.m takes the form:

$$\frac{\partial}{\partial \bar{t}}\mathbf{G}^<(\bar{t},\bar{\omega}) = i\left[\mathbf{G}^<(\bar{t},\bar{\omega}),\mathbf{h}_0\right] + i\int d\omega'[\mathbf{G}^<(\bar{t},\bar{\omega}+\omega')\mathbf{v}(\bar{t},\omega') - \mathbf{v}(\bar{t},\omega')\mathbf{G}^<(\bar{t},\bar{\omega}-\omega')], \tag{11}$$

where $\mathbf{v}(\bar{t},\bar{\omega})$ is the mixed representation of the time dependent contribution to the Hamiltonian, $\mathbf{v}(\bar{t})$, and can be expressed in terms of the Fourier transformed form ($\tilde{\mathbf{v}}(\omega) = \mathcal{F}[\mathbf{v}(t)]$):

$$\mathbf{v}(\bar{t},\bar{\omega}) = \frac{1}{\pi} e^{-i2\bar{\omega}\bar{t}} \int_{-\infty}^{\infty} dt e^{i(2\bar{\omega})t} \mathbf{v}(t) = \frac{1}{\pi} e^{-i2\bar{\omega}\bar{t}} \tilde{\mathbf{v}}(2\bar{\omega}). \tag{12}$$

This mixed time-frequency representation of the responding electronic system, as used below, provides substantial physical insight into the electronic response aspects of the propagated model system.[65]

2.3. Propagating the electrode-coupled system

The infinite nature of the coupled system is represented by adding bulk self-energies as shown next. Here $\bar{\mathbf{h}}_0$, $\bar{\mathbf{v}}(\bar{t},\omega')$ and $\bar{\mathbf{G}}^<(\bar{t},\bar{\omega})$ are in the AO representation and $\mathbf{S}$ is the AO overlap matrix. We parse the system's model space into a device region and two bulk regions.

$$\bar{\mathbf{h}}_0 = \begin{bmatrix} \bar{\mathbf{h}}_{0LL} & \bar{\mathbf{h}}_{0LC} & 0 \\ \bar{\mathbf{h}}_{0CL} & \bar{\mathbf{h}}_{0CC} & \bar{\mathbf{h}}_{0CR} \\ 0 & \bar{\mathbf{h}}_{0RC} & \bar{\mathbf{h}}_{0RR} \end{bmatrix} \tag{13}$$

$$\bar{\mathbf{S}} = \begin{bmatrix} \bar{\mathbf{S}}_{LL} & 0 & 0 \\ 0 & \bar{\mathbf{S}}_{CC} & 0 \\ 0 & 0 & \bar{\mathbf{S}}_{RR} \end{bmatrix} \tag{14}$$

$$\bar{\mathbf{v}}(t,\omega) = \begin{bmatrix} 0 & 0 & 0 \\ 0 & \bar{\mathbf{v}}_{CC}(t,\omega) & 0 \\ 0 & 0 & 0 \end{bmatrix} \tag{15}$$

$$\bar{\mathbf{G}}^<(\bar{t},\bar{\omega}) = \begin{bmatrix} \bar{\mathbf{G}}^<_{LL}(\bar{t},\bar{\omega}) & \bar{\mathbf{G}}^<_{LC}(\bar{t},\bar{\omega}) & 0 \\ \bar{\mathbf{G}}^<_{CL}(\bar{t},\bar{\omega}) & \bar{\mathbf{G}}^<_{CC}(\bar{t},\bar{\omega}) & \bar{\mathbf{G}}^<_{CR}(\bar{t},\bar{\omega}) \\ 0 & \bar{\mathbf{G}}^<_{RC}(\bar{t},\bar{\omega}) & \bar{\mathbf{G}}^<_{RR}(\bar{t},\bar{\omega}) \end{bmatrix} \tag{16}$$

We next solve for the bulk-coupled lesser GF in the mixed representation ($\bar{\mathbf{G}}^<_{CC}(\bar{t},\bar{\omega})$):

$$\begin{aligned} i\frac{\partial}{\partial\bar{t}}\mathbf{G}^<_{CC}(\bar{t},\bar{\omega}) &= \left[\mathbf{h}_{0CC}, \mathbf{G}^<_{CC}(\bar{t},\bar{\omega})\right] \\ &+ \sum_{I\in L,R} \left[\mathbf{h}_{CI}\mathbf{G}^<_{IC}(\bar{t},\bar{\omega}) - \mathbf{G}^<_{CI}(\bar{t},\bar{\omega})\mathbf{h}_{IC}\right] \\ &+ \int d\omega' [\mathbf{v}_{CC}(\bar{t},\omega')\mathbf{G}^<_{CC}(\bar{t},\bar{\omega}-\omega') - \mathbf{G}^<_{CC}(\bar{t},\bar{\omega}+\omega')\mathbf{v}_{CC}(\bar{t},\omega')]. \end{aligned} \tag{17}$$

$$\begin{aligned} i\frac{\partial}{\partial\bar{t}}\mathbf{G}^<_{IC}(\bar{t},\bar{\omega}) &= \mathbf{h}_{0II}\mathbf{G}^<_{IC}(\bar{t},\bar{\omega}) + \mathbf{h}_{0IC}\mathbf{G}^<_{CC}(\bar{t},\bar{\omega}) \\ &- \mathbf{G}^<_{II}(\bar{t},\bar{\omega})\mathbf{h}_{0IC} - \mathbf{G}^<_{IC}(\bar{t},\bar{\omega})\mathbf{h}_{0CC} \\ &- \int d\omega' [\mathbf{G}^<_{IC}(\bar{t},\bar{\omega}+\omega')\mathbf{v}_{CC}(\bar{t},\omega')]. \end{aligned} \tag{18}$$

where $I \in L, R$. Furthermore, given the assumptions made on the overlap matrix, we have $\mathbf{v}_{CC}(\bar{t},\omega') = \mathbf{S}_{CC}^{-1/2}\bar{\mathbf{v}}_{CC}(\bar{t},\omega')\mathbf{S}_{CC}^{-1/2}$, $\mathbf{h}_{0IJ} = \mathbf{S}_{II}^{-1/2}\bar{\mathbf{h}}_{0IJ}\mathbf{S}_{JJ}^{-1/2}$ and $\mathbf{G}^<_{IJ}(\bar{t},\bar{\omega}) = \mathbf{S}_{II}^{1/2}\bar{\mathbf{G}}^<_{IJ}(\bar{t},\bar{\omega})\mathbf{S}_{JJ}^{1/2}$ for $I, J \in L, C, R$.

We now divide the lesser GF into a sum of two parts:

$$\mathbf{G}^<(\bar{t},\bar{\omega}) \equiv \mathbf{G}^{0,<}(\bar{\omega}) + \mathbf{\Delta}\mathbf{G}^<(\bar{t},\bar{\omega}) \tag{19}$$

where $\mathbf{G}^{0,<}(\bar{\omega})$ is the lesser GF in the absence of a TD perturbation (i.e. Hamiltonian is constant in time, see discussion proceeding equation (2)) and $\mathbf{\Delta G}^{<}(\bar{t},\bar{\omega})$ is the remainder (i.e. the part that carries all perturbation effects). This implies that

$$\frac{\partial}{\partial \bar{t}}\mathbf{G}^{0,<}(\bar{\omega}) = 0 \tag{20}$$

and therefore,

$$\frac{\partial}{\partial \bar{t}}\mathbf{G}^{<}(\bar{t},\bar{\omega}) = \frac{\partial}{\partial \bar{t}}\mathbf{\Delta G}^{<}(\bar{t},\bar{\omega}) \tag{21}$$

Using these properties and the approximations above, we can rewrite eqns. (17) and (18) in terms of $\mathbf{\Delta G}^{<}(\bar{t},\bar{\omega})$:

$$\begin{aligned} i\frac{\partial}{\partial \bar{t}}\mathbf{\Delta G}^{<}_{CC}(\bar{t},\bar{\omega}) &= \left[\mathbf{h}_{0CC}, \mathbf{\Delta G}^{<}_{CC}(\bar{t},\bar{\omega})\right] \\ &+ \sum_{I\in L,R}\left[\mathbf{h}_{CI}\mathbf{\Delta G}^{<}_{IC}(\bar{t},\bar{\omega}) - \mathbf{\Delta G}^{<}_{CI}(\bar{t},\bar{\omega})\mathbf{h}_{IC}\right] \\ &+ \int d\omega'[\mathbf{v}_{CC}(\bar{t},\omega')\mathbf{G}^{0,<}_{CC}(\bar{\omega}-\omega') - \mathbf{G}^{0,<}_{CC}(\bar{\omega}+\omega')\mathbf{v}_{CC}(\bar{t},\omega')] \\ &+ \int d\omega'[\mathbf{v}_{CC}(\bar{t},\omega')\mathbf{\Delta G}^{<}_{CC}(\bar{t},\bar{\omega}-\omega') - \mathbf{\Delta G}^{<}_{CC}(\bar{t},\bar{\omega}+\omega')\mathbf{v}_{CC}(\bar{t},\omega')]\,, \end{aligned} \tag{22}$$

$$i\frac{\partial}{\partial \bar{t}}\mathbf{\Delta G}^{<}_{IC}(\bar{t},\bar{\omega}) = \mathbf{h}_{0II}\mathbf{\Delta G}^{<}_{IC}(\bar{t},\bar{\omega}) - \mathbf{\Delta G}^{<}_{IC}(\bar{t},\bar{\omega})\mathbf{h}_{0CC} + \mathbf{h}_{0IC}\mathbf{\Delta G}^{<}_{CC}(\bar{t},\bar{\omega})\,. \tag{23}$$

We integrate these equations after redefining $\mathbf{\Delta G}^{<}_{IC}(\bar{t},\bar{\omega})$ as follows:

$$\mathbf{\Delta G}^{<}_{IC}(\bar{t},\bar{\omega}) \equiv e^{-i\mathbf{h}_{0II}(\bar{t}-t_0)}\mathbf{\Delta}\mathcal{G}^{<}_{IC}(\bar{t},\bar{\omega})e^{i\mathbf{h}_{0CC}(\bar{t}-t_0)}. \tag{24}$$

Upon substitution of definition eqn. 24 into eqn. 23 we get,

$$\mathbf{\Delta G}^{<}_{IC}(\bar{t},\bar{\omega}) = \int_{-\infty}^{\bar{t}} d\bar{t}' e^{i\mathbf{h}_{0II}(\bar{t}'-\bar{t})}\mathbf{h}_{0IC}\mathbf{\Delta G}^{<}_{CC}(\bar{t},\bar{\omega})e^{-i\mathbf{h}_{0CC}(\bar{t}'-\bar{t})} \tag{25}$$

Note that the integration lower bound is set at $-\infty$ because unlike $\mathbf{v}(t)$ which starts at some finite t_0, $\mathbf{v}(\bar{t},\bar{\omega})$ is potentially infinite in extent. Equation 25 together with the property $\mathbf{\Delta G}^{<\dagger}_{IC}(\bar{t},\bar{\omega}) = -\mathbf{\Delta G}^{<}_{CI}(\bar{t},\bar{\omega})$ can be substituted into equation 22 to give

$$\begin{aligned} i\frac{\partial}{\partial \bar{t}}\mathbf{\Delta G}^{<}_{cc}(\bar{t},\bar{\omega}) &= \left[\mathbf{h}_{cc}, \mathbf{\Delta G}^{<}_{cc}(\bar{t},\bar{\omega})\right] + \int d\omega'[\mathbf{v_{cc}}(\bar{t},\omega')\mathbf{G}^{<}_{cc}(\bar{t},\bar{\omega}-\omega') - \mathbf{G}^{<}_{cc}(\bar{t},\bar{\omega}+\omega')\mathbf{v_{cc}}(\bar{t},\omega')] \\ &+ \int_{-\infty}^{\bar{t}} dt'[\mathbf{\Sigma^R}(\bar{t}-t')\mathbf{\Delta G_{cc}}^{<}(t',\bar{\omega})e^{-i\mathbf{h_{cc}}(\bar{t}-t')} - e^{i\mathbf{h_{cc}}(\bar{t}-t')}\mathbf{\Delta G_{cc}}(t',\bar{\omega})\Sigma^A(t'-\bar{t})], \end{aligned} \tag{26}$$

where the self energies $\mathbf{\Sigma^R}(t)$ and $\mathbf{\Sigma^A}(t)$ are defined as follows:

$$\mathbf{\Sigma^R}(t) \equiv \sum_{I\in L,R}\mathbf{h}_{0CI}\mathbf{g^R_{II}}(t)\mathbf{h}_{0IC} \tag{27}$$

$$\mathbf{\Sigma^A}(t) \equiv \sum_{I\in L,R}\mathbf{h}_{0CI}\mathbf{g^A_{II}}(t)\mathbf{h}_{0IC} \tag{28}$$

$$\mathbf{g}^{\mathbf{R}}_{\mathbf{II}}(t) \equiv -i\Theta(t)e^{-i\mathbf{h}_{\mathbf{II}}t} \tag{29}$$

$$\mathbf{g}^{\mathbf{A}}_{\mathbf{II}}(t) \equiv i\Theta(-t)e^{-i\mathbf{h}_{\mathbf{II}}t} \tag{30}$$

with $\Theta(-t)$ the Heaviside step function.

For description of TD conductance the electronic density at the unperturbed state has to be properly evaluated as the initial conditions of the propagation. The initial $\mathbf{G}^{0,<}$ (*i.e.* the unperturbed equilibrated system) must describe well the steady state, which is thermally equilibrated with the electron baths. We remind that in the physically proper non-partitioned view[107] the different subsystems are allowed to reach thermal equilibration as one system. Namely, their coupling is not part of the turned on perturbation.[59, 60, 66]

2.4. Equilibrated Initial Conditions

The Keldysh formalism is used next to properly account for the thermal equilibration of the device with the electrodes and its affect on $G^<$. A Matsubara GF (G^M) corresponds entirely to the imaginary part of the KC and is used to describe the system at thermal equilibrium. Through KC continuation

$$G^M \rightarrow G^<(t_0, t_0) \equiv G^<_0. \tag{31}$$

In the absence of a perturbation, $\mathbf{G}^<(\bar{t}, \bar{\omega}) = \mathbf{G}^{\mathbf{0},<}(\bar{\omega}) = \mathbf{G}^{\mathbf{0},<}_{\mathbf{1}}(\bar{\omega}) - \mathbf{G}^{\mathbf{0},<\dagger}_{\mathbf{1}}(\bar{\omega})$, where

$$\mathbf{G}^{\mathbf{0},<}_{\mathbf{1}}(\bar{\omega}) = i\mathbf{G}^{\mathbf{R}}(\bar{\omega})\mathbf{G}^<_{\mathbf{0}} = -\mathbf{G}^{\mathbf{R}}(\bar{\omega})\mathbf{f}(\mathbf{h_0} - \mu I). \tag{32}$$

The Fermi-matrix $\mathbf{f}(\mathbf{A})$ is a function of a matrix and in the limit of non-interacting electrons is given by $\mathbf{f}(\mathbf{A}) = e^{-\beta\mathbf{A}}\left[\mathbf{I} + e^{-\beta\mathbf{A}}\right]^{-1}$, assuming $\mathbf{A}$ is Hermitian. This condition is satisfied for the orthogonalized basis set, where $\mathbf{h_0} = \mathbf{S^{-1/2}}\bar{\mathbf{h}}\mathbf{S^{-1/2}}$. The Fermi-matrix above provides an analytical solution for the Matsubara GF ($\mathbf{G^M}$) in the case of non-interacting electrons.

More specifically, we evaluate the unperturbed system in the localized basis, whereas the propagation relations are all implemented in the orthogonalized representation. For a Hamiltonian of a closed system represented in a finite basis, $\mathbf{G}^{0,<}(\bar{\omega})$ is diagonal in the basis that diagonalizes $\bar{\mathbf{h}}$. This implies that $\mathbf{G}^{0,<}(\bar{\omega})$ does not introduce any off-diagonal coherences. On the other hand, an open system introduces a non-trivial $\bar{\omega}$ dependence to the Hamiltonian (through the bulk SEs). In this case, the initial guess is still guaranteed not to correspond to arbitrarily turning on the electron density of the leads at $\bar{t} = t_0$, since $\bar{\omega}$ depends on all Δt.

2.5. Propagating using frequency domain bulk self-energy

Next, the projected equation (eq. 26) is written in the integrated form, where $\mathbf{h}_{cc}$ is diagonalized becomes

$$\begin{aligned} i\Delta G^<_{cc,ij}(\bar{t}, \bar{\omega}) = \\ \int_{-\infty}^{\infty} \Theta(\bar{t} - t')e^{-i\Delta\epsilon_{ij}(\bar{t}-t')} \left\{ \int d\omega' [\mathbf{v_{cc}}(t', \omega')\mathbf{G}^<_{cc}(t', \bar{\omega} - \omega') - \mathbf{G}^<_{cc}(t', \bar{\omega} + \omega')\mathbf{v_{cc}}(t', \omega')]_{ij} \right\} \\ + \int_{-\infty}^{\infty} \Theta(\bar{t} - t')e^{-i\Delta\epsilon_{ij}(\bar{t}-t')} \int_{-\infty}^{\infty} dt'' \sum_{k,l} [\Gamma_{ijkl}(t' - t'')\Delta G^<_{cc,kl}(t'', \bar{\omega})]. \end{aligned} \tag{33}$$

In equation (33), $\int_{-\infty}^{\bar{t}} dt' \rightarrow \int_{-\infty}^{\infty} dt'\Theta(\bar{t} - t')$ and the electrodes are described by a memory kernel of the form

$$\Gamma_{ijkl}(t) \equiv \Sigma^R_{ik}(t)e^{i\epsilon_j t}\delta_{lj} - \Sigma^A_{lj}(-t)e^{-i\epsilon_i t}\delta_{ik}. \tag{34}$$

We then proceed to express the e.o.m.s in the two-frequency representation by an additional Fourier transform (FT):

$$\boldsymbol{G}^{<}(\Delta\omega,\bar{\omega}) \equiv \int_{-\infty}^{\infty} d\bar{t} e^{i\Delta\omega\bar{t}} \boldsymbol{G}^{<}(\bar{t},\bar{\omega}). \tag{35}$$

Applying the Fourier transform to eqn. 33 gives

$$\begin{aligned}\Delta G^{<}_{CC,ij}(\Delta\omega,\bar{\omega}) = \mathcal{G}_{ij}(\Delta\omega)\left[\tilde{\mathbf{v}}_{CC}(\Delta\omega)\mathbf{G}^{0,<}_{CC}(\bar{\omega}-\Delta\omega/2) - \mathbf{G}^{0,<}_{CC}(\bar{\omega}+\Delta\omega/2)\tilde{\mathbf{v}}_{CC}(\Delta\omega)\right]_{ij} \\ +\frac{1}{\pi}\mathcal{G}_{ij}(\Delta\omega)\int d\omega'\left[\tilde{\mathbf{v}}_{CC}(2\omega')\boldsymbol{\Delta G}^{<}_{CC}(\bar{\omega}-\omega',\Delta\omega-2\omega') - \boldsymbol{\Delta G}^{<}_{CC}(\bar{\omega}+\omega',\Delta\omega-2\omega')\tilde{\mathbf{v}}_{CC}(2\omega')\right]_{ij} \\ +\mathcal{G}_{ij}(\Delta\omega)\sum_{k,l}\Gamma_{ijkl}(\Delta\omega)\Delta G^{<}_{cc,kl}(\Delta\omega,\bar{\omega}),\end{aligned} \tag{36}$$

where

$$\Gamma_{ijkl}(\Delta\omega) \equiv \int dt e^{i\Delta\omega t}\Gamma_{ijkl}(t) = \Sigma^{R}_{ik}(\epsilon_j+\Delta\omega)\delta_{lj} - \Sigma^{A}_{lj}(\epsilon_i-\Delta\omega)\delta_{ik}. \tag{37}$$

In addition, we use, as routinely employed, a small broadening factor η in defining the propagator to enhance the stability of the solution:

$$\mathcal{G}_{ij}(\Delta\omega) = \frac{1}{\Delta\omega + i\eta - \Delta\epsilon_{ij}}. \tag{38}$$

This broadening ensures that eventually (at $t \to \infty$) the system will return to its initial equilibrium configuration. In practice, any finite grid method in the frequency domain requires an artificial broadening to resolve infinitesimally narrow peaks. The final result is

$$\begin{aligned}\sum_{k,l}\boldsymbol{\mathcal{H}}_{ijkl}(\Delta\omega)\boldsymbol{\Delta G}^{<}_{CC,kl}(\Delta\omega,\bar{\omega}) = \left[\tilde{\mathbf{v}}_{CC}(\Delta\omega)\mathbf{G}^{0,<}_{CC}(\bar{\omega}-\Delta\omega/2) - \mathbf{G}^{0,<}_{CC}(\bar{\omega}+\Delta\omega/2)\tilde{\mathbf{v}}_{CC}(\Delta\omega)\right]_{ij} \\ +\frac{1}{\pi}\int d\omega'\left[\tilde{\mathbf{v}}_{CC}(2\omega')\boldsymbol{\Delta G}^{<}_{CC}(\bar{\omega}-\omega',\Delta\omega-2\omega') - \boldsymbol{\Delta G}^{<}_{CC}(\bar{\omega}+\omega',\Delta\omega-2\omega')\tilde{\mathbf{v}}_{CC}(2\omega')\right]_{ij},\end{aligned} \tag{39}$$

where

$$\boldsymbol{\mathcal{H}}_{ijkl}(\Delta\omega) \equiv (\Delta\omega + i\eta - \Delta\epsilon_{ij})\delta_{ik}\delta_{jl} - \Gamma_{ijkl}(\Delta\omega). \tag{40}$$

The final result can be Fourier transformed back to the mixed representation to generate Wigner type information that provides important insight on the quantum mechanical effects that determine the time-dependence of the observable (*i.e.* the current operator).

We note that eqn. 39 involves a tensor of rank four that operates on a matrix (tensor of rank 2). Consequently, we employ tetradic notation to re-expresses matrices as vectors and rank four tensors as matrices. Using this notation an $n \times n$ matrix $\mathbf{A}$ with elements A_{ij} is rewritten as a vector $|A\rangle\rangle$ with elements $|A\rangle\rangle_{ni+j}$. Likewise, a tensor $\mathcal{H}$ with element $\mathcal{H}_{ijkl}$ (where i,j,k,l each spans over n elements) is rewritten as an $n^2 \times n^2$ matrix $\mathbf{H}$, with elements $\mathbf{H}_{ni+j,nk+l}$. The tetradic notation for eqn. 39 takes the form:

$$\mathbf{H}(\Delta\omega)|\boldsymbol{\Delta G}^{<}_{CC}(\Delta\omega,\bar{\omega})\rangle\rangle = |B^{(1)}_{CC}(\Delta\omega,\bar{\omega})\rangle\rangle + \frac{1}{\pi}\int d\omega'|B_{CC}(\omega',\Delta\omega,\bar{\omega})\rangle\rangle, \tag{41}$$

where

$$\mathbf{H}_{ni+j,nk+l}(\Delta\omega) \equiv \boldsymbol{\mathcal{H}}_{ijkl}(\Delta\omega), \tag{42}$$

$$|\mathbf{\Delta G}^{<}_{CC}(\Delta\omega,\bar{\omega})\rangle\rangle_{ni+j} \equiv \mathbf{\Delta G}^{<}_{CC,ij}(\Delta\omega,\bar{\omega}), \tag{43}$$

$$|B^{(1)}_{CC}(\Delta\omega,\bar{\omega})\rangle\rangle_{ni+j} \equiv \left[\tilde{\mathbf{v}}_{CC}(\Delta\omega)\mathbf{G}^{0,<}_{CC}(\bar{\omega}-\Delta\omega/2) - \mathbf{G}^{0,<}_{CC}(\bar{\omega}+\Delta\omega/2)\tilde{\mathbf{v}}_{CC}(\Delta\omega)\right]_{ij} \tag{44}$$

and

$$\begin{aligned} |B_{CC}(\omega',\Delta\omega,\bar{\omega})\rangle\rangle_{ni+j} \equiv \\ \left[\tilde{\mathbf{v}}_{CC}(2\omega')\mathbf{\Delta G}^{<}_{CC}(\bar{\omega}-\omega',\Delta\omega-2\omega') - \mathbf{\Delta G}^{<}_{CC}(\bar{\omega}+\omega',\Delta\omega-2\omega')\tilde{\mathbf{v}}_{CC}(2\omega')\right]_{ij}. \end{aligned} \tag{45}$$

Finally inverting $\mathbf{H}(\Delta\omega)$ gives

$$|\mathbf{\Delta G}^{<}_{CC}(\Delta\omega,\bar{\omega})\rangle\rangle = \mathbf{G}(\Delta\omega)|B^{(1)}_{CC}(\Delta\omega,\bar{\omega})\rangle\rangle + \frac{1}{\pi}\mathbf{G}(\Delta\omega)\int d\omega'|B_{CC}(\omega',\Delta\omega,\bar{\omega})\rangle\rangle, \tag{46}$$

where

$$\mathbf{G}(\Delta\omega) \equiv \mathbf{H}^{-1}(\Delta\omega). \tag{47}$$

In this notation, a tensor equation appears as a matrix equation and all matrix operations (multiplication, inversion, diagonalization, etc.) can be applied to the rexpressed equation of motion.

The final expression can be formally expanded to n-th order in the perturbation $\tilde{\mathbf{v}}(\Delta\omega)$. In this expansion, we express the TD electronic density in terms of the evolving occupations of the projected device states. The band structure due to the coupling to the electrodes is included directly in the expansion through the energy distribution variable ($\bar{\omega}$) that is also used to calculate the SEs. In the results reported below we study transient current that is appropriately treated at the first order. We also study the effect of initial conditions that include an established non-equilibrium steady state in response to an applied constant bias. We describe next the form of the solution for the steady state case.

2.6. Steady state limit of the perturbative expansion

We now discuss the solution for the steady state, where a constant bias has been turned on for a long time. The Fourier transform of a time independent perturbation $\mathbf{v}(t) = \mathbf{v}_\circ$ (as in eqn. 35) takes the following form in the frequency domain

$$\tilde{\mathbf{v}}(\Delta\omega) = 2\pi\delta(\Delta\omega)\mathbf{v}_\circ. \tag{48}$$

The resulting two-frequency representation of the time-dependent equations of motion is used to derive the time-independent correction to $G^{0,<}$. In this scheme, time independent fields (such as a source-drain bias that has been turned on for a long time) are treated exactly by specializing eqn. 41.

Implementing this scheme for the steady state and without loss of generality, the perturbing potential $\mathbf{v}(t)$ is rewritten as the sum of a time-independent field (of arbitrary strength) $\mathbf{v}_\circ$ and a time dependent perturbing field $\mathbf{v}_{TD}(t)$. Fourier transforming to the frequency domain gives

$$\tilde{\mathbf{v}}(\Delta\omega) = 2\pi\delta(\Delta\omega)\mathbf{v}_\circ + \tilde{\mathbf{v}}_{TD}(\Delta\omega). \tag{49}$$

The resulting two-frequency equation of motion becomes

$$\mathbf{H}_{v_\circ}(\Delta\omega)|\mathbf{\Delta G}^{<}_{TD,CC}(\Delta\omega,\bar{\omega})\rangle\rangle = |B^{(1)}_{TD,CC}(\Delta\omega,\bar{\omega})\rangle\rangle + \frac{1}{\pi}\int d\omega'|B_{TD,CC}(\omega',\Delta\omega,\bar{\omega})\rangle\rangle, \tag{50}$$

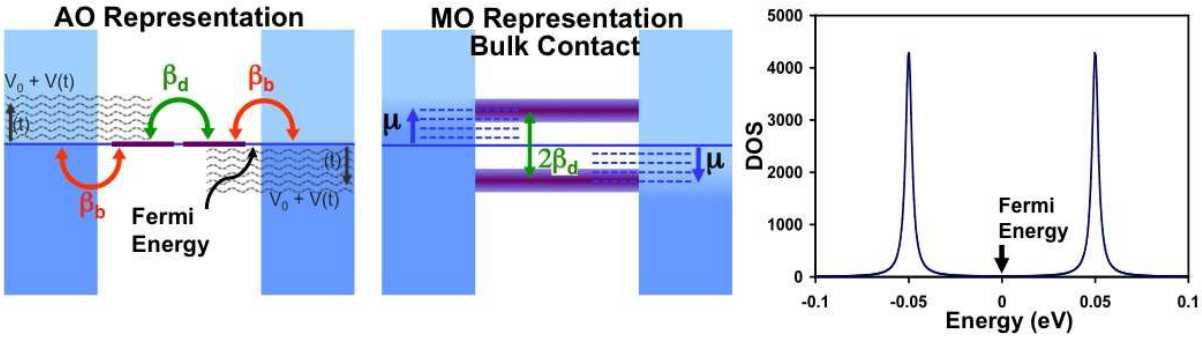

Figure 1. Schematic diagram of the model system. (a) localized/atomic orbital representation, where the strong coupling of the device state to the wires are indicated (b) Diagonalized molecular orbital representation. (c) Broadened electronic density of states.

where the propagating super operator

$$\mathbf{H}_{v_\circ,ni+j,nk+l}(\Delta\omega) \equiv \boldsymbol{\mathcal{H}}_{ijkl}(\Delta\omega) - (v_{\circ,ik}\delta_{lj} - v_{\circ,lj}\delta_{ik}) \tag{51}$$

includes the steady perturbation. The total lesser Green function is now defined in terms of a new time independent initial guess $G^{0,<}_{v_\circ}$ that includes the effects of the time-independent field exactly. In the absence of additional time-dependent perturbations, $G^{0,<}_{v_\circ}$ is the total lesser Green function for the system. The remainder, $\Delta G^<_{TD}$, is related to the time dependent perturbations

$$|\boldsymbol{\Delta G}^<_{TD,CC}(\Delta\omega,\bar{\omega})\rangle\rangle \equiv |G^<_{CC}(\Delta\omega,\bar{\omega})\rangle\rangle - 2\pi\delta(\Delta\omega)|G^{0,<}_{v_\circ,CC}(\bar{\omega})\rangle\rangle, \tag{52}$$

where

$$|G^{0,<}_{v_\circ,CC}(\bar{\omega})\rangle\rangle = |G^{0,<}_{CC}(\bar{\omega})\rangle\rangle + \mathbf{G}_{v_\circ}(0)|B^{(1)}_{v_\circ,CC}(\bar{\omega})\rangle\rangle. \tag{53}$$

Here, $\mathbf{G}_{v_\circ}(\Delta\omega) = \mathbf{H}^{-1}_{v_\circ}(\Delta\omega)$ and

$$|B^{(1)}_{v_\circ,CC}(\bar{\omega})\rangle\rangle_{ni+j} \equiv \left[\mathbf{v}_{\circ,CC}\mathbf{G}^{0,<}_{CC}(\bar{\omega}) - \mathbf{G}^{0,<}_{CC}(\bar{\omega})\mathbf{v}_{\circ,CC}\right]_{ij}. \tag{54}$$

Now, the time dependent "B"-terms are rewritten in terms of the modified initial guess $G^{0,<}_{v_\circ}$ and the time-dependent components of the perturbation ($v_{TD}(\Delta\omega)$):

$$|B^{(1)}_{TD,CC}(\Delta\omega,\bar{\omega})\rangle\rangle_{ni+j} \equiv \left[\tilde{\mathbf{v}}_{TD,CC}(\Delta\omega)\mathbf{G}^{0,<}_{v_\circ,CC}(\bar{\omega}-\Delta\omega/2) - \mathbf{G}^{0,<}_{v_\circ,CC}(\bar{\omega}+\Delta\omega/2)\tilde{\mathbf{v}}_{TD,CC}(\Delta\omega)\right]_{ij} \tag{55}$$

and

$$|B_{TD,CC}(\omega',\Delta\omega,\bar{\omega})\rangle\rangle_{ni+j} \equiv \left[\tilde{\mathbf{v}}_{TD,CC}(2\omega')\boldsymbol{\Delta G}^<_{TD,CC}(\Delta\omega-2\omega',\bar{\omega}-\omega') - \boldsymbol{\Delta G}^<_{TD,CC}(\bar{\omega}+\omega',\Delta\omega-2\omega')\tilde{\mathbf{v}}_{TD,CC}(2\omega')\right]_{ij}. \tag{56}$$

The last two equations are identical in form to the general equations (44) and (45). In these equations the effect of $\mathbf{v}_\circ$ enters explicitly only into the Hamiltonian super operator, where we replace $\mathbf{H}(\Delta\omega)$ with $\mathbf{H}_{v_\circ}(\Delta\omega)$ and the initial lesser GF ($G^{0,<}$) with $G^{0,<}_{v_\circ}$. We emphasize that the constant perturbation cannot be simply added to the Hamiltonian for calculating the initial lesser Green function $G^{0,<}(\bar{\omega})$ for proper description of existing non-equilibrium conditions. The effect of a source-drain bias on an initially decoherent electronic charge density cannot be modeled by a simple field asymmetry embedded within the Hamiltonian.

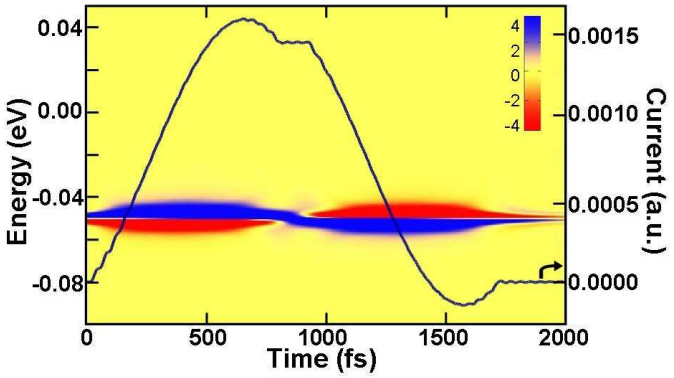

Figure 2. The transient current under the effect of a slowly varying potential. Both the corresponding current density is provided (band structure at the ground state). Note that the right axis corresponds to the current curve while the left axis corresponds to the energy distribution variable

2.6.1. Current evaluation We now describe the evaluation of the current from the time propagated $G^<$ function. The grand canonical expectation value of any dynamical variable (following the KC formalism[104, 106, 108]) is given by

$$\langle \hat{J}(t_1) \rangle = -i \int_{-\infty}^{\infty} d\vec{x}_1 \lim_{x_2 \to x_1} \left[\mathcal{J}(\vec{x}_1) G^<(x_1, x_2) \right] . \tag{57}$$

The expectation value can be expressed as a product of two matrices

$$\begin{aligned} \langle \mathbf{J}(t_1) \rangle = -iTr \left[\lim_{t_2 \to t_1} \left[\mathcal{O}\mathbf{G}^<(t_1, t_2) \right] \right] = -iTr \left[\lim_{\Delta t \to 0, \bar{t} \to t_1} \left[\mathcal{J}\mathbf{G}^<(\bar{t}, \Delta t) \right] \right] = \\ Tr \left[\lim_{\bar{t} \to t_1} \left[\frac{-i}{2\pi} \int_{-\infty}^{\infty} d\bar{\omega} \mathcal{J}\mathbf{G}^<(\bar{t}, \bar{\omega}) \right] \right] , \end{aligned} \tag{58}$$

where $\mathcal{J}_{\mathbf{ij}} = \int_{-\infty}^{\infty} \mathbf{d\tilde{x}} \phi_{\mathbf{i}}(\tilde{\mathbf{x}}) \mathcal{J}(\tilde{\mathbf{x}}) \phi_{\mathbf{j}}(\tilde{\mathbf{x}})$. Let us now consider the specific case of the current density operator:

$$\mathcal{J}(\vec{x}) = -i \left[\vec{\nabla}_x \delta(\vec{x} - \vec{r}) + \delta(\vec{x} - \vec{r}) \vec{\nabla}_x \right] \tag{59}$$

or in an AO basis representation

$$\mathcal{J}_{ji}(\vec{r}) = i \left[\phi_i(\vec{r}) \vec{\nabla} \phi_j(\vec{r}) - \phi_j(\vec{r}) \vec{\nabla} \phi_i(\vec{r}) \right] . \tag{60}$$

The electron current through a given plane is calculated by tracing $[-i\mathcal{J}\mathbf{G}^<]$.

2.6.2. Models We concentrate in this study on the transient current through a one dimensional wire composed of hopping sites, where interactions are included only between neighboring sites. In the considered model, the confined system includes two states which are coupled strongly by β_d to result with a pair of bonding and anti-bonding states separated by $2\beta_d$ ($H_{12} = H_{21} \equiv \beta_d$, where H is the electronic Hamiltonian). This energy level scheme is illustrated in Figure 1, where the atomic orbital representation is provided in part (a) and the corresponding MO picture reflecting the coupling is given in part (b). The two strongly inter-coupled orbitals are interfaced with electrodes to result with a pair of conducting (broadened) bands of states. In

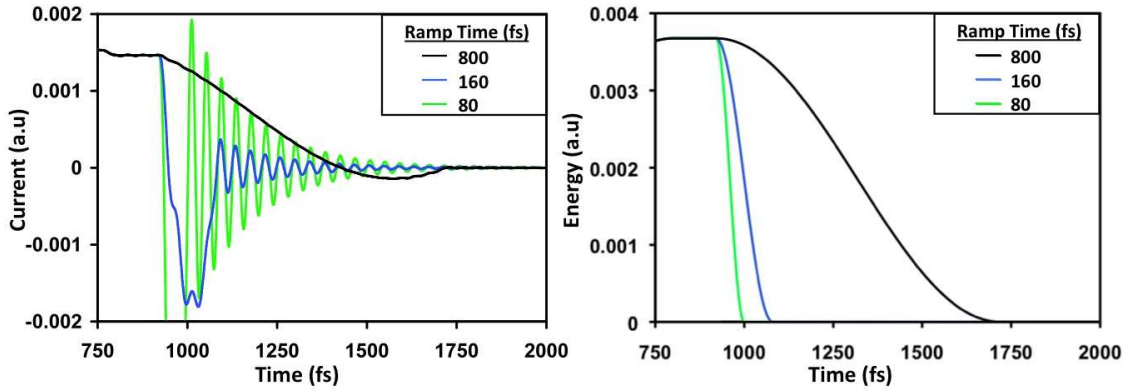

Figure 3. TD currents which differ in the rate of the potential turn off. The 3 TD bias curves are provided to the right.

the AO representation this is achieved by coupling each site of the strongly interacting pair to a different lead. The coupling to the leads is represented by the SEs, $\Sigma = \beta_c^{\dagger} g_s \beta_c$. In our model, the surface GF (g_s) is an imaginary constant number that implements a wide band approximation for the electronic density of the bulk material projected on the surface site. We use $\beta_d = -0.005(eV), \beta_c = 0.1\beta_d$ where the resulting density of states (DOS) is plotted in part (c).

We note that β and s are the electronic and overlap coupling terms. The diagonal terms of the model Hamiltonian are set to the initial Fermi energy of the system. Accordingly, we express the current operator with the numerical values assigned to the electronic integrals in the Hamiltonian

$$\mathbf{J} = \mathbf{i} \begin{bmatrix} 0 & \beta_d \\ -\beta_d & 0 \end{bmatrix}. \tag{61}$$

The traced quantity $i\mathbf{J}\mathbf{G}^{<}(\bar{\mathbf{t}}, \bar{\omega})$ provides the TD band structure (energy distibution) of the current operator. In this case it describes the evolving current through the center of the model system. In all calculations reported below in the results section we set the FE to zero ($\mu_0 = 0$). This also defines the on site energies as described in the figure.

We use a sufficiently small value ($\eta_d = 0.002eV$) for the broadening factor added to the imaginary component of the Hamiltonian used to calculate the G^R of the equilibrated system (eq 32). Finally, we note that in all calculations the target bias potential is set to 0.1V unless otherwise stated.

3. Results

We begin by considering the effect of a direct current (DC) potential bias, where we follow the switching temporal effect on the transient current. The current following a (relatively) slow rate for switching off the bias is provided in Figure 2. (Note the current scale is provided to the right). We note that while the switching off time is long, where an oscillatory transient response is almost absent, the transient current dips below zero before the full dissipation of the system to the zero current limit. We then further resolve the time-dependence of the band structure of the current operator. The figure depicts, by a projected color map, the distribution of the current operator ($J(\bar{\omega}, \bar{t})$), where the current at any time can be extracted by integrating over the energy distribution ($\int d\bar{\omega} J(\bar{\omega}, \bar{t})$). The current is associated with contributions from the lower occupied state (ground state), where the upper portion of the band contributes to the positive current. The band structure of the current operator at the switch off is the reflection

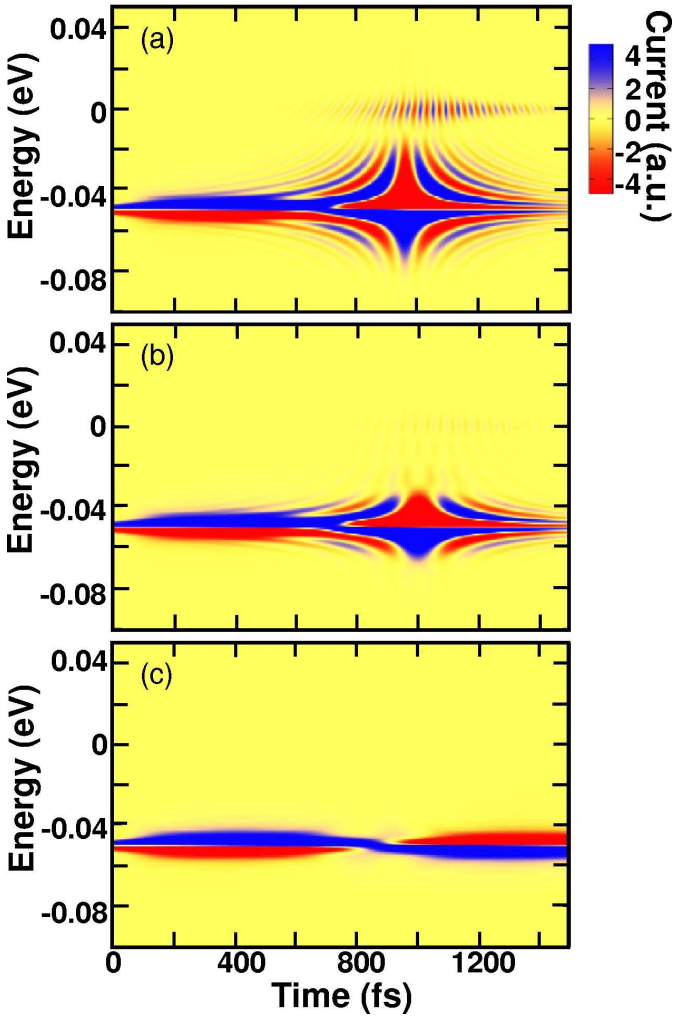

Figure 4. Time-dependent current distributions projected on a color map (I(t) are provided in Figure 3). (a) fastest turn off rate, (b) medium turn off rate, (c) slowest turn off rate.

of the band at the turn on event. At turn off, the positive part of the distribution is at the energetically lower part of the band (further away from the Fermi energy). The band narrows, as the current continues to dissipate.

The current under increased rates of bias switching is considered next. In Figure 3 we provide the current upon varying the rate for switching off the bias. The oscillatory response of the current is shown to increase in amplitude with the rate of switching. It is also evident that the current will oscillate with a larger number of periods when the rate is increased. This is also reflected in the band structure as shown in Figure 4. The oscillatory response is shown to be related to the direct interference of the two states. The quicker rate of the turn off is shown to result in stronger interference due to the two states. The frequency of the oscillation depends on the present energy levels, where the amplitude of the oscillation is determined by the rate of perturbation change.

We now clarify that the temporal features of the current distribution prior to the switching off as indicated in the figure is not a violation of causality. This is related to the nature of the $\bar{t}$ variable, and by taking the full distribution we generate information that is dependent on

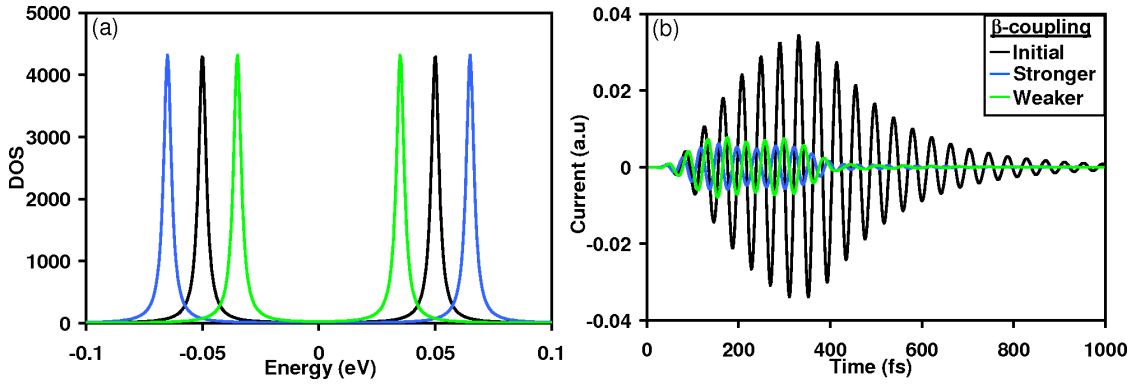

Figure 5. Effect of the coupling strength: (a) The density of states (b) TD current under an AC tuned to the original coupling strength.

the observational time. Indeed, the current operator, which serves as physical probe, illustrates that causality is preserved. This can also be understood as a reflection of the uncertainty principle, where Husimi transformations can be used to reflect the fundamental limitations of measurements. This highlights the importance in the current distributions expressed in Wigner form as further demonstrated below. This representation is used to analyze the underlying quantum effects leading to the oscillatory and directed response of the current.

As apparent by the current distribution due to the quick switching event, the two states can be coupled to interfere and lead to an oscillatory response of the current. Stronger coherence can clearly be achieved by a monochromatic field that is tuned to oscillate at a frequency associated to the energy separating the two energy levels. In Figure 5 we follow the effect of a tuned driving AC bias on the current. The AC amplitude is at 0.01V. We apply an AC pulse tuned exactly to the weakly coupled states and then apply the same AC bias on the two states where their coupling is either enhanced or decreased by 30% relative to the orignal value. The change in the coupling strength, as reflected in Figure 5 (a), either further separates (increased β_d) or diminishes the energy gap between the two states (reduced β_d). In either case, as shown in Figure 5 (b), the responding current oscillations are reduced. The case where the energy levels are further separated leads to a reduced time period of the response (increase of the frequency). This is expected from the nature of the coupling-induced detuning effect. We note that upon the opposite shift in β the period is slightly increasing.

The coherence underlying the response to an AC bias is also reflected in the band structure of the current operator. In Figure 6 the color maps for the current plots of Figure 5 are provided. We follow the effect of varying the coupling strength where the AC remains tuned exactly to the system with the original β coupling parameter. The current band structure of the perfectly tuned case (unshifted β_d) demonstrates the strong amplitude of the AC response by the straight (vertical) bands. These bands are slanted at the transient conditions as shown in Figure 6 (a). For the β detuned cases as shown in Figures 6 (b-c) the slanting is increased and the conductance amplitudes are diminished as expected. The mini-band that appears at a shift below the populated state due to the interference with the excited state depends on the tuning. The detuning diminishes its strength and shifts its location. It is shifted below -0.1eV for the case with the stronger coupling or above that value for the second detuned case. Finally, we also point at the different features of the detuning due to the change in beta as reflected, for example, in the decay regime of the main coherence, see Figures 6 (b-c).

We next consider the effect of a DC bias on a coherent driven system, where the frequency of the applied AC bias is set exactly to the energy difference between the two levels. The effect of

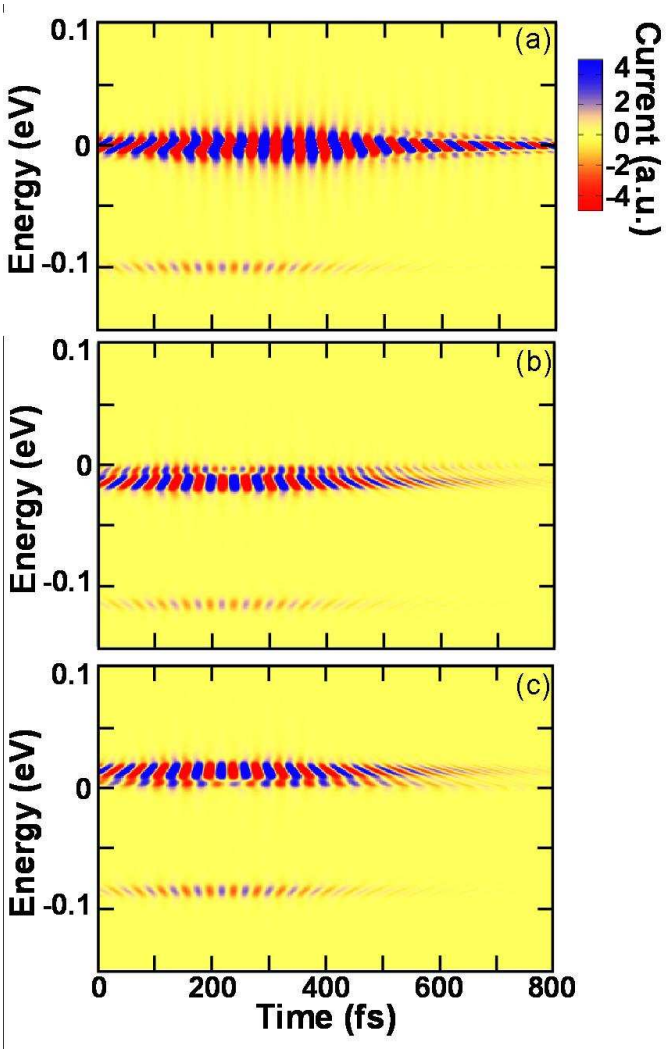

Figure 6. The current band structure corresponding to the AC tuned to the energy difference of the two energy levels under the effect of varying the coupling strength (see Figure 5). (a) initial coupling , (b) stronger coupling, (c) weaker coupling.

the DC bias to detune the response was analyzed before[65]. Here its effect to shift the electronic spectra is demonstrated in Figure 7 (a). The electronic excitation energy is shown to increase due to the DC bias as expected. The applied DC bias also further broadens the spectral peak and diminishes its height. In Figures 7 (b-d) we follow the TD currents with different strengths of an applied DC under the effect of an AC bias that is retuned to the DC affected energy states. The three plots focus each on different time ranges, where Figure 7 (b) provides an overall view, Figure 7 (c) zooms on the initial times where the existing conducting flux is evident. It is also demonstrated that the flux due to the DC bias reduces the amplitude of the oscillatory response, an effect that can be studied only by a TD scheme. Finally Figure 7 (d) shows the tail, where the AC bias is turned off and the system returns to its constant biased state.

The band structure of the corresponding current operator is provided in Figure 8. The effect of the bias to induce constant flux is reflected in the thin band centered about the ground state energy that is enhanced by the increase of the DC bias. As expected the main coherence is

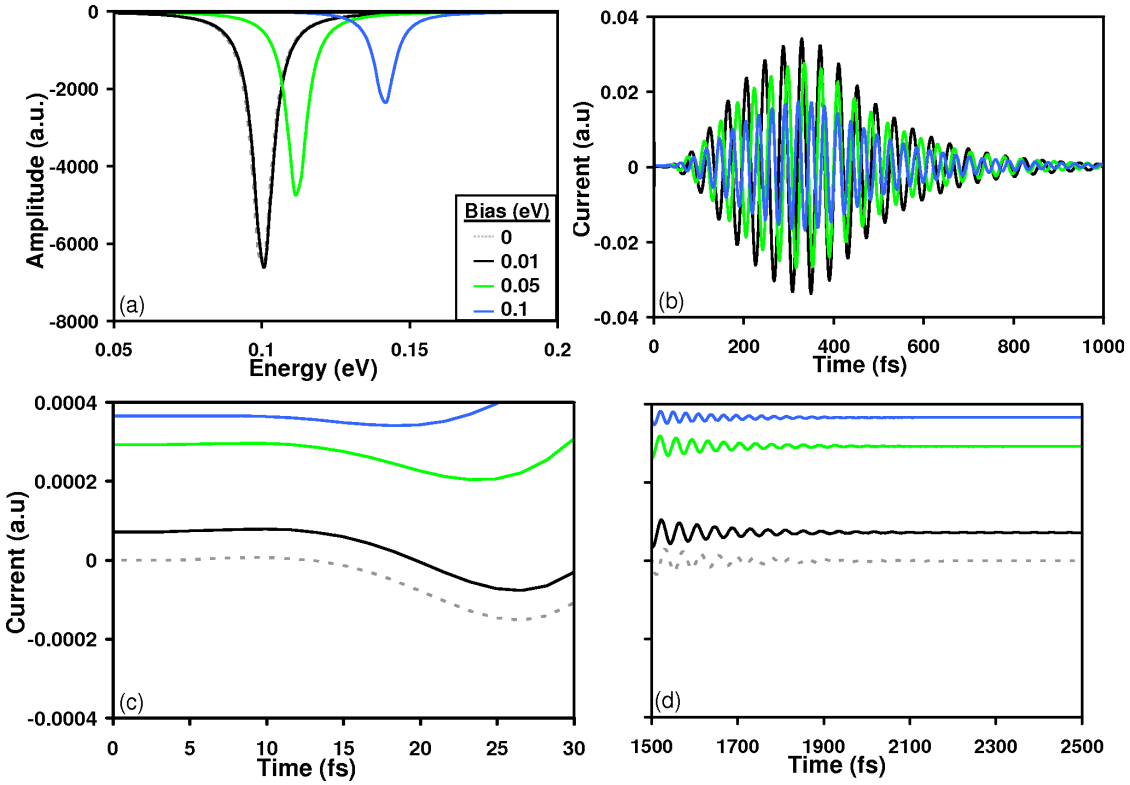

Figure 7. Effects of an existing DC bias on: (a) Electronic spectra of the bias system (b-d) Coherence driven conductance.

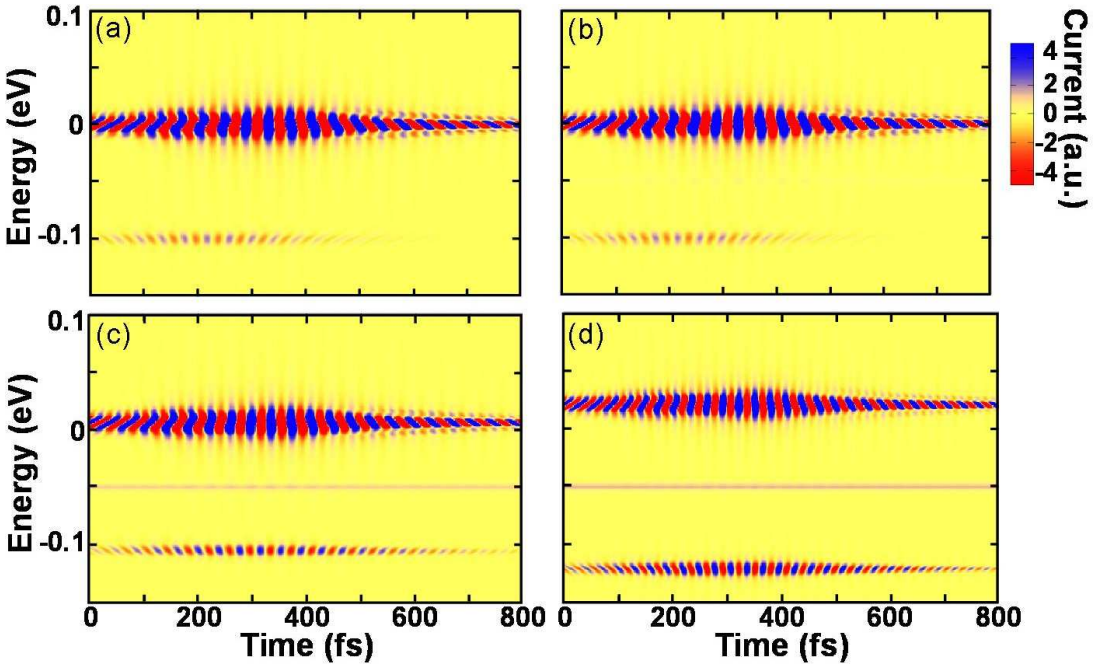

Figure 8. The current distributions of the cases with different applied DC biases. (a) 0 eV, (b) 0.01 eV, (c) 0.05 eV, (d) 0.10 eV.

obtained at the energy exactly between the two interfering states. This main coherence is shown to decrease, in spite of the retuning of the AC bias, in the presence of the DC induced flux. This is a consequence of the DC to reduce the spectral peak that corresponds to the electronic excitation as revealed above. Interestingly, the mini-band of the current operator corresponding to the shift below the ground state features an opposite trend. This mini-band is somewhat enhanced upon the application of the bias. This effect however is still not able to reverse the overall observation of the DC bias reducing the oscillatory response.

4. Concluding Comments

Electron transport through model electronic channels is studied by solving the electronic equations of motion of coupled and bias systems. The electronic equations of motion is represented using Keldysh formalism by Green Functions. Their solution is obtained by expressing the time dependence in the frequency domain, where in order to achieve full time resolution the GFs are defined using two independent time variables. We solve the equations using TD perturbation theory.

The TD approach provides a rigorous treatment of the extended system. The calculations also provide a plethora of information through the resolved band structure of the evolving electronic density. Here, the band structure of the current operator in model electronic channels are solved for. The study considers the transient features of the transport through biased systems. The evolving current operator is used to generate data that highlights the quantum interferences that determine the oscillatory current at transient conditions. The oscillatory component of the current that is noted at transient conditions is associated with interference of the conducting states, where the constant component under steady state conditions when the transient features are dissipated is determined by the broadening extent of the conducting states.

The TD approach is also used to study driven transport. In the considered system, the oscillatory bias perturbation affects the current through the state interferences. The relationships between DC bias and AC-inducing coherences are studied in detail. The calculated current operator is used to reflect the quantum interferences affecting the current under the driving TD perturbations. The ability to analyze in general the possibility for driving the current by applied TD perturbations becomes of increased importance due to experimental related advances.

Acknowledgments

BDD acknowledges University of Michigan and the Petroleum Research Fund of the ACS (through Grant 47118-G6) for financial support. HP would like to acknowledge the University of Michigan Rackham Graduate School Summer Institute for financial support.

References

[1] Bumm L A, Arnold J J, Cygan M T, Dunbar T D, Burgin T P, Jones L I, Allara D L, Tour J M and Weiss P S 1996 *Science* **271** 1705–1707
[2] Reed M A, Zhou C, Muller C J, Burgin T P and Tour J M 1997 *Science* **278** 252–254
[3] Stipe B C, Rezaei M A and Ho W 1998 *Science* **280** 1732–1735
[4] Chen J, Reed M A, Rawlett A M and Tour J M 1999 *Science* **286** 1550–1552
[5] Collier C P, Wong E W, Belohradsky M, Raymo F M, Stoddart J F, Kuekes P J, Williams R S and Heath J R 1999 *Science* **285** 391–394
[6] Park H, Park J, Lim A K L, Anderson E H, Alivisatos A P and McEuen P L 2000 *Nature* **407** 57–60
[7] Collier C P, Mattersteig G, Wong E W, Luo Y, Beverly K, Sampaio J, Raymo F M, Stoddart J F and Heath J R 2000 *Science* **289** 1172–1175
[8] Rueckes T, Kim K, Joselevich E, Tseng G Y, Cheung C L and Lieber C M 2000 *Science* **289** 94–97
[9] Joachim C, Gimzewski J K and Aviram A 2000 *Nature* **408** 541–548
[10] Collins P G, Arnold M S and Avouris P 2001 *Science* **292** 706–709

[11] Holmlin R E, Haag R, Chabinyc M L, Ismagilov R F, Cohen A E, Terfort A, Rampi M A and Whitesides G M 2001 *J. Am. Chem. Soc.* 5075–5085
[12] Cui X D, Primak A, Zarate X, Tomfohr J, Sankey O F, Moore A L, Moore T A, Gust D, Harris G and Lindsay S M 2001 *Science* **294** 571–574
[13] Nitzan A 2001 *Annu. Rev. Phys. Chem.* **52** 681
[14] Tour J M, Rawlett A M, Kozaki M, Yao Y X, Jagessar R C, Dirk S M, Price D W, Reed M A, Zhou C W, Chen J, Wang W Y and Campbell I 2001 *Chem.-Eur. J.* **7** 5118–5134
[15] Reichert J, Ochs R, Beckmann D, Weber H B, Mayor M and v Löhneysen H 2002 *Phys. Rev. Lett.* **88** 176804
[16] Kushmerick J G, Holt D B, Pollack S K, Ratner M A, Yang J C, Schull T L, Naciri J, Moore M H and Shashidhar R 2002 *J. Am. Chem. Soc.* **124** 10654–10655
[17] Mbindyo J K N, Mallouk T E, Mattzela J B, Kratochvilova I, Razavi B, Jackson T N and Mayer T S 2002 *jacs*
[18] Fan F R F, Yang J P, Cai L T, Price D W, Dirk S M, Kosynkin D V, Yao Y X, Rawlett A M, Tour J M and Bard A J 2002 *J. Am. Chem. Soc.* **124** 5550–5560
[19] Park J, Pasupathy A N, Goldsmith J I, Chang C, Yaish Y, Petta J R, Rinkoski M, Sethna J P, Abruna H D, McEuen P L and Ralph D C 2002 *Nature* **417** 722–725
[20] Liang W J, Shores M P, Bockrath M, Long J R and Park H 2002 *Nature* **417** 725–729
[21] Luo Y, Collier C P, Jeppesen J O, Nielsen K A, Delonno E, Ho G, Perkins J, Tseng H R, Yamamoto T, Stoddart J F and Heath J R 2002 *ChemPhysChem* **3** 519
[22] Adams D M, Brus L, Chidsey C E D, Creager S, Creutz C, Kagan C R, Kamat P V, Lieberman M, Lindsay S, Marcus R A, Metzger R M, Michel-Beyerle M E, Miller J R, Newton M D, Rolison D R, Sankey O, Schanze K S, Yardley J and Zhu X Y 2003 *J. Phys. Chem. B* **107** 6668–6697
[23] Metzger R M 2003 *Chem. Rev.* **103** 3803–3834
[24] Nazin G V, Qiu X H and Ho W 2003 *Science* **302** 77–81
[25] Nitzan A and Ratner M A 2003 *Science* **300** 1384–1389
[26] Xu B Q and Tao N 2003 *Science* **301** 1221–1223
[27] Kushmerick J, Lazorcik J, Patterson C, Shashidhar R, Seferos D and Bazan G 2004 *Nano. Lett.* **4** 639–642
[28] Xiao X, Xu B Q and Tao N 2004 *Nano. Lett.* **4** 267–271
[29] Xiao X, Xu B Q and Tao N 2004 *Angew. Chem. Int. Ed.* **45** 6148–6152
[30] Guisinger N, Greene M, Basu R, Baluch A and Hersam M 2004 *Nano. Lett.* **4** 55–59
[31] McCreery R L 2004 *Chem. Mater.* 4477–4496
[32] Fan F R, Yao Y, Cai L, Cheng L, Tour J and Bard A 2004 *Journal of the American Chemical Society* **126** 4035–4042 ISSN 0002-7863
[33] Piva P G, DiLabio G A, Pitters J L, Zikovsky J, Rezeq M, Dogel S, Hofer W A and Wolkow R A 2005 *Nature* **435** 658–661
[34] Xu B Q, Xiao X Y, Yang X, Zang L and Tao N J 2005 *J. Am. Chem. Soc.* **127** 2386–2387
[35] Kitagawa K, Morita T and Kimura S 2005 *J. Phys. Chem. B* **109** 13906–13911
[36] Guo X, Small J P, Klare J E, Wang Y, Purewal M S, Tam I W, Hong B H, Caldwell R, Huang L, O'Brien S, Yan J, Breslow R, Wind S J, Hone J, Kim P and Nuckolls C 2006 *Science* **311** 356–359
[37] Natelson D, Yu L H, Ciszek J W and Keane Z K T J M 2006 *Chem. Phys* **324** 267–275
[38] Keane Z K, Ciszek J W, Tour J M and Natelson D 2006 *Nano. Lett.* **6** 1518–1521
[39] Zhirnov V V and Cavin R K 2006 *Nat. Mater.* **5** 11–12
[40] Tang J, Wang Y, Nuckolls C and Wind S J 2006 *J. Vac. Sci. Technol. B.* **24** 3227–3229
[41] Tang J Y, Wang Y L, Klare J E, Tulevski G S, Wind S J and Nuckolls C 2007 *Angew. Chem. Int. Ed.* **46** 3892–3895
[42] Venkataraman L, Park Y S, Whalley A C, Nuckolls C, Hybertsen M S and Steigerwald M L 2007 *Nano. Lett.* **7** 502–506 ISSN 1530-6984
[43] Chen F, Hihath J, Huang Z, Li X and J T N 2007 *Annu. Rev. Phys. Chem.* **58** 535–564
[44] Chen X, Jeon Y M, Jang J W, Qin L, Huo F, Wei W and Mirkin C A 2008 *J. Am. Chem. Soc.* 8166–8188
[45] Ashwell G J, Wierzchowiec P, Phillips L J, Collins C J, Gigon J, Robinson B J, Finch C M, Grace I R, Lambert C J, Buckle P D, Ford K, Wood B J and Gentle I R 2008 *Phys. Chem. Chem. Phys.* **10** 1859–1866 URL `http://dx.doi.org/10.1039/b719417j`
[46] Kouwenhoven L P, Jauhar S, Orenstein J, McEuen P L, Nagamune Y, Motohisa J and Sakaki H 1994 *Phys. Rev. Lett.* **73** 3443–3446
[47] van der Vaart N C, Godijn S F, Nazarov Y V, Harmans C J P M, Mooij J E, Molenkamp L W and Foxon C T 1995 *Phys. Rev. Lett.* **74** 4702–4705
[48] Keay B J, Zeuner S, Allen S J, Maranowski K D, Gossard A C, Bhattacharya U and Rodwell M J W 1995 *Phys. Rev. Lett.* **75** 4102–4105

[49] Oosterkamp T H, Kouwenhoven L P, Koolen A E A, van der Vaart N C and Harmans C J P M 1997 *Phys. Rev. Lett.* **78** 1536–1539
[50] López R, Aguado R, Platero G and Tejedor C 1998 *Phys. Rev. Lett.* **81** 4688–4691
[51] Brouwer P W 1998 *Phys. Rev. B* **58** R10135–R10138
[52] Oosterkamp T H, Fujisawa T, van der Wiel W G, Ishibashi K, Hijman R V, Tarucha S and Kouwenhoven L P 1998 *Nature* **395** 873–876
[53] Switkes M, Marcus C M, Campman K and Gossard A C 1999 *Science* **283** 1905–1908
[54] Zhou F, Spivak B and Altshuler B 1999 *Phys. Rev. Lett.* **82** 608–611
[55] Nordlander P, Pustilnik M, Meir Y, Wingreen N S and Langreth D C 1999 *Phys. Rev. Lett.* **83** 808–811
[56] Platero G and Aguado R 2004 *Phys. Reports* **395** 1–157
[57] Murphy J E, Beard M C and Nozik A J 2006 *J. Phys. Chem. B* **110** 25455–25461
[58] Zhong Z, Gabor N M, Sharping J E, Gaeta A L and MCeuen P L 2008 *Nature Nanotechnology* **3** 201
[59] Stefanucci G and Almbladh C O 2004 *Phys. Rev. B* **69** 195318–195334
[60] Kurth S, Stefanucci G, Almbladh C O, Rubio A and Gross E K U 2005 *Phys. Rev. B* **72** 035308
[61] Bushong N, Sai N and Di Ventra M 2005 *Nano. Lett.* **5** 2569
[62] Maciejko J, Wang J and Guo H 2006 *Phys. Rev. B* **74** 085324
[63] Hou D, He Y, Liu X, Kang J, Chen J and Han R 2006 *Physica E* **31** 191
[64] Sai N, Bushong N, Hatcher R and Ventra M D 2007 *Phys. Rev. B* **75** 115410 (pages 8)
[65] Prociuk A and Dunietz B D 2008 *Phys. Rev. B* **78** 165112
[66] Stefanucci G, Kurth S, Rubio A and Gross E K U 2008 *Phys. Rev. B* **77** 075339
[67] Kouwenhoven L P, Jauhar S, McCormick K, Dixon D, McEuen P L, Nazarov Y V, van der Vaart N C and Foxon C T 1994 *Phys. Rev. B* **50** 2019–2022
[68] Nowak A M and McCreery R L 2004 *J. Am. Chem. Soc.* **126** 16621–16631
[69] Nowak A M and McCreery R L 2004 *Analytical Chemistry* **76** 1089–1097
[70] Bonifas A P and McCreery R L 2008 *Chemistry of Materials* **20** 3849–3856
[71] Ward D R, Halas N J, Ciszek J W, Tour J M, Wu Y, Nordlander P and Natelson D 2008 *Nano. Lett.* **8** 919–924
[72] Ward D R, Scott G D, Keane Z K, Halas N J and Natelson D 2008 *J. Phys.: Condens. Matter* **20** 374118
[73] Stoof T H and Nazarov Y V 1996 *Phys. Rev. B* **53** 1050–1053
[74] Stafford C A and Wingreen N S 1996 *Phys. Rev. Lett.* **76** 1916–1919
[75] Brune P, Bruder C and Schoeller H 1997 *Phys. Rev. B* **56** 4730–4736
[76] Pedersen M H and Büttiker M 1998 *Phys. Rev. B* **58** 12993–13006
[77] Wang B, Wang J and Guo H 1999 *Phys. Rev. Lett.* **82** 398–401
[78] Moskalets M and Büttiker M 2004 *Phys. Rev. B* **69** 205316
[79] Arrachea L 2005 *Phys. Rev. B* **72** 121306
[80] Wu B H and Cao J C 2006 *Phys. Rev. B* **73** 205318
[81] Agarwal A and Sen D 2007 *Physical Review B (Condensed Matter and Materials Physics)* **76** 235316 (pages 7)
[82] Arrachea L, Naon C and Salvay M 2007 *Phys. Rev. B* **76** 165401
[83] Baer R and Neuhauser D 2003 *Int. J. Quant. Chem.* **91** 524–532
[84] Baer R, Seidman T, Ilani S and Neuhauser D 2004 *J. Chem. Phys.* **120** 3387–3396
[85] Baer R and Neuhauser D 2004 *J. Chem. Phys.* **121** 9803–9807
[86] Burke K, Car R and Gebauer R 2005 *Phys. Rev. Lett.* **94** 146803
[87] Neuhauser D and Baer R 2005 *J. Chem. Phys.* **123** 204105
[88] Qian X, Ju Li J, Lin X and Yip S 2006 *Phys. Rev. B* **73** 035408
[89] Zheng X, Wang F, Yam C Y, Mo Y and Chen G 2007 *Phys. Rev. B* **75** 195127
[90] Gurvitz S A and Prager Y S 1996 *Phys. Rev. B* **53** 15932–15943
[91] Lehmann J, Kohler S, Hänggi P and Nitzan A 2002 *Phys. Rev. Lett.* **88** 228305
[92] Lehmann J, Kohler S, Hanggi P and Nitzan A 2003 *The Journal of Chemical Physics* **118** 3283–3293
[93] Torres L E F F 2005 *Phys. Rev. B* **72** 245339
[94] Harbola U, Esposito M and Mukamel S 2006 *Phys. Rev. B* **74** 235309
[95] Moskalets M and Büttiker M 2002 *Phys. Rev. B* **66** 205320
[96] Moskalets M and Büttiker M 2004 *Phys. Rev. B* **70** 245305
[97] Jauho A P, Wingreen N S and Meir Y 1994 *Phys. Rev. B* **50** 5528–5544
[98] You J Q, Lam C H and Zheng H Z 2000 *Phys. Rev. B* **62** 1978–1983
[99] Zhu Y, Maciejko J, Ji T, Guo H and Wang J 2005 *Phys. Rev. B* **71** 075317 (pages 10)
[100] Arrachea L and Moskalets M 2006 *Phys. Rev. B* **74** 245322 (pages 13)
[101] Arrachea L, Yeyati A L and Martin-Rodero A 2008 *Physical Review B (Condensed Matter and Materials Physics)* **77** 165326 (pages 8)

[102] Baym G 1961 *Physical Review* **124** 287
[103] Baym G 1962 *Physical Review* **127** 1391
[104] Kadanoff L P and Baym G 1962 *Quantum Statistical Mechanics* (New York: Benjamin and Cummings)
[105] Langreth D C 1976 *Linear and Non-linear Electron Transport in Solids* (New-York: Plenum Press)
[106] Bonitz M 1998 *Quantum Kinetic Theory* (Stuttgart: Teubner)
[107] Cini M 1980 *Phys. Rev. B* **22** 5887
[108] Fetter A L and Walecka J D 2003 *Quantum Statistical Mechanics* (Dover)
[109] Prociuk A, Van Kuiken B and Dunietz B D 2006 *J. Chem. Phys.* **125** 204717